

## ***Ginkgo biloba* leaf extract for the synthesis of gold nanoparticles and its application for electrochemical detection of diclofenac**

Zemin Li, Shuyan Xiang, Yin Pan and Li Fu\*

Key Laboratory of Novel Materials for Sensor of Zhejiang Province, College of Materials and Environmental Engineering, Hangzhou Dianzi University, Hangzhou 310018, China

\*E-mail: [fuli@hdu.edu.cn](mailto:fuli@hdu.edu.cn)

Received: 1 July 2022 / Accepted: 4 August 2022 / Published: 10 September 2022

---

In this work, gold nanoparticles were prepared by reduction using *Ginkgo biloba* extract and modified with a glassy carbon electrode to investigate the electrochemical behavior of diclofenac. The effect of temperature on the synthesis of gold nanoparticles was investigated. The results showed that the best gold nanoparticles were synthesized at 180 °C. SEM characterized the prepared gold nanoparticles, and the size distribution was about 50~100 nm. During the electrochemical detection of diclofenac, two experimental parameters, the modification amount and the sweep rate were optimized, and a modification amount of 5  $\mu\text{L}$  and a sweep rate of 100 mV/s were determined. The performance of the green synthesized gold nanoparticle modified electrode for the electrochemical detection of diclofenac was investigated using cyclic voltammetry with linear detection limits ranging from 5 to 600  $\mu\text{M}$  and the lowest detection limit of 0.524  $\mu\text{M}$ . In addition, the effect of impurity ions (molecules) on the electrochemical detection of diclofenac at gold nanoparticle-modified electrodes was investigated, and the results showed that none of the impurities measured affected the qualitative detection of diclofenac.

---

**Keywords:** Nanomaterials; *Ginkgo biloba*; Gold nanoparticles; Diclofenac; Electrochemical detection

### **1. INTRODUCTION**

Nanomaterials have some unique characteristics due to their small size, such as quantum size effect, small size effect, etc. Metal nanomaterials are widely used in electronic devices, medical devices, and other fields and have become a preferred material for preparing related devices [1]. Currently, the mainstream preparation methods of nanomaterials are mainly physical, chemical, and biological. Physical methods are generally more expensive to prepare and usually consume more energy. Chemical methods usually use some toxic and harmful agents, which may cause pollution to the environment [2]. In contrast, the biological method has many advantages: low cost, easy collection of raw materials, safety, and environmental friendliness [3].

Taib et al. [4] prepared gold nanoparticles using a green synthesis of aqueous extract of *Hibiscus sabdariffa* leaves. They identified chlorogenic acid in *Hibiscus sabdariffa* leaves as the main antioxidant compound involved in reducing Au<sup>3+</sup> ions. They compared the electrocatalytic activity of bare GCE and Au-NPs/GCE for nitrite electrooxidation by cyclic voltammetry test. Gold nanoparticles were synthesized using *Lonicera japonica* extract by Maheshkumar et al.[5] The synthesis of gold nanoparticles was confirmed from the color change (light yellow to ruby color) and UV-Vis spectra (absorbance 530-580 nm). The size of the synthesized gold nanoparticles was derived by characterization to be about 10-40 nm, mostly spherical, with a few triangular and hexagonal shapes. Their experimental results showed that the gold nanoparticles synthesized using *Lonicera japonica* extract could inhibit the growth of cervical cancer cells and be used to treat cervical cancer. Balasubramanian et al. [6] prepared gold nanoparticles by green reduction using *Jasminum auriculatum* leaf extract and performed several characterization and studies. After characterization, it was concluded that the synthesized gold nanoparticles were spherical, with an average size of 8-37 nm. They were subjected to pH stability studies using PBS buffer solution. The results showed that the gold nanoparticles have good compatibility in biomedicine and have significant antibacterial effects against various human pathogenic bacteria. Using extracts of plant tissues (e.g., roots, stems, leaves, seeds, fruits, etc.) as reducing and stabilizing agents is one of the most popular choices in the preparation of metal nanoparticles by biomethod reduction [7–9]. *Ginkgo biloba* L. is the only species under Ginkgoopsida, an ancient and rare species of Mesozoic relics [10,11]. Therefore, it is genetically stable and does not have natural hybridization, making it a suitable research object for refining and exploring plant extracts to synthesize nanoparticles.

Diclofenac is a commonly used non-steroidal anti-inflammatory drug with anti-inflammatory, analgesic, and antipyretic effects. It is often used clinically for the treatment and relief of pain caused by various types of arthritis and various kinds of neuralgia [12,13]. Diclofenac plays an important role in clinical applications, but it is ecologically damaging and may cause mutations in the kidneys and fins of some fish and also tends to enrich fish and other organisms [14,15]. It is not only a direct ecological hazard but also an indirect one. For example, the Indian condor has suffered mass mortality from consuming animals enriched with diclofenac [16]. The degradation rate of diclofenac in the natural environment is relatively low, and the efficiency of conversion degradation by natural microbial action is also very low. There are also many studies on diclofenac, such as the photodegradation mechanism of diclofenac in a simulated natural light environment and the catalytic degradation of diclofenac using modified titanium dioxide nanotubes, and the study of the adsorption removal process of diclofenac [17–20]. In this work, diclofenac's electrochemical behavior will be investigated using the prepared gold nanomaterials modified with glassy carbon electrodes.

## 2. EXPERIMENTAL

### 2.1. Reagents and instruments

*Ginkgo biloba* leaves were collected from the living area of Hangzhou Dianzi University. Anhydrous ethanol, disodium hydrogen phosphate, potassium dihydrogen phosphate were purchased

from Shanghai Aladdin Biochemical Technology Co. Diclofenac and chloroauric acid were purchased from Shanghai Maclean Biochemical Technology Co. Glucose was purchased from Tianjin Yongda Chemical Reagent Co. Ascorbic acid was purchased from Sinopharm Group Chemical Reagent Co. Uric acid was purchased from Shanghai Source Leaf Biotechnology Co. Laboratory prepared solutions of potassium chloride/potassium ferricyanide,  $\text{Co}^{2+}$ ,  $\text{Ni}^{2+}$ ,  $\text{Zn}^{2+}$ ,  $\text{Cu}^{2+}$ ,  $\text{Mn}^{2+}$ ,  $\text{F}^-$ ,  $\text{CH}_3\text{COO}^-$ ,  $\text{SO}_4^{2-}$  were used directly in the experiment.

A CHI-760E Electrochemical Workstation (Shanghai Chenhua Instrument Co., LTD.) has been used for electrochemical experiments. A three-electrode system was used in the experiment, with a glassy carbon electrode as the working electrode, a platinum plate as the counter electrode, and Ag/AgCl (saturated KCl) as the reference electrode. The morphology of the samples was observed by a scanning electron microscope (Apreo S, Thermo Fisher Scientific, USA).

## 2.2. Preparation of gold nanoparticles and investigation of the effect of temperature on gold nanoparticles

Preparation of *Ginkgo biloba* extract: A certain amount of *Ginkgo biloba* leaves were washed to remove dust and cut up. Using water as solvent, the leaves were further crushed using a high throughput tissue grinder. After allowing it to stand for some time, the supernatant was taken. The supernatant was centrifuged using a tabletop high-speed centrifuge to remove the fine leaf residue to obtain *Ginkgo biloba* extract.

In preparation of gold nanoparticles synthesized at different temperatures: 5 mL of *Ginkgo biloba* extract was taken and added to the reaction kettle, and then 100  $\mu\text{L}$  of 0.1 M chloroauric acid was added. The reaction kettle was placed in a pre-heated drying oven for 4 h. Six temperatures were set: 30  $^\circ\text{C}$ , 60  $^\circ\text{C}$ , 90  $^\circ\text{C}$ , 120  $^\circ\text{C}$ , 150  $^\circ\text{C}$ , and 180  $^\circ\text{C}$ .

Comparison of the performance of the green synthesized gold nanoparticle modified electrodes at different temperatures: The glassy carbon electrodes were modified with the six prepared *Ginkgo biloba* extract-gold nanoparticle mixture solutions synthesized at different temperatures (5  $\mu\text{L}$  of solution), and their performance was examined in potassium chloride/potassium ferricyanide solution using cyclic voltammetry (CV) and electrochemical impedance spectroscopy (EIS).

Comparison of the performance of the green synthetic gold nanoparticle modified electrode at different temperatures for the detection of diclofenac: The glassy carbon electrode was modified with the six prepared *Ginkgo biloba* extract-gold nanoparticle mixture solutions synthesized at different temperatures (5  $\mu\text{L}$  of solution), and 100  $\mu\text{L}$  of diclofenac solution with a concentration of 10 mM in 2 mL PBS buffer solution (the actual concentration of diclofenac detected was 500  $\mu\text{M}$ ) was added to the CV.

## 2.3. Parameter Optimization

The parameters were optimized for the amount of modification: a mixed solution of *Ginkgo biloba* extract-gold nanoparticles was added dropwise to the surface of the glassy carbon electrode, and

the water was dried in a drying oven at a temperature of 60 °C to immobilize the gold nanomaterials on the electrode surface. The modified glassy carbon electrode was used as the working electrode for detecting diclofenac. The experiments were performed at 0 µL, 1 µL, 3 µL, 5 µL, 7 µL, 9 µL, 10 µL, 15 µL, 20 µL and 25 µL of modifier solution.

Parameter optimization of the scan rate: Diclofenac was still detected using CV with three-electrode detection. Ten scan rates were set, from 20 mV/s to 200 mV/s, with a sweep rate interval of 20 mV/s. The relationship between peak current and scan rate was further analyzed at the end of the measurement.

#### 2.4. Detection limits of diclofenac by cyclic voltammetry at nanogold-modified electrodes

Different concentrations of diclofenac were assayed by CV (the solution to be tested was 5 mL of PBS solution + different amounts of different concentrations of diclofenac solutions). Nineteen concentrations were measured from low to high concentrations: 0.01 µM, 0.05 µM, 0.1 µM, 0.5 µM, 1 µM, 5 µM, 10 µM, 20 µM, 40 µM, 60 µM, 80 µM, 100 µM, 200 µM, 300 µM, 400 µM, 500 µM, 600 µM, 700 µM, 800 µM. After the measurement, the peak current versus concentration was further analyzed to find the linear detection range, and the detection limits were calculated.

#### 2.5. Interference and effect of impurity ions (molecules) on the detection of diclofenac at modified electrodes

The impurity molecule solutions: glucose, ascorbic acid, and uric acid were used as interfering molecules. In addition, the experiment was set up to detect five cations of  $\text{Co}^{2+}$ ,  $\text{Ni}^{2+}$ ,  $\text{Zn}^{2+}$ ,  $\text{Cu}^{2+}$ ,  $\text{Mn}^{2+}$ , and three anions of  $\text{F}^-$ ,  $\text{CH}_3\text{COO}^-$ , and  $\text{SO}_4^{2-}$  (eight impurity ions have been prepared in the laboratory at a concentration of 2 g/L), for a total of 11 substances. Among them, the cation and anion detection concentration is about 30-fold that of diclofenac. The detection concentration of uric acid is about 20-fold that of diclofenac. The detection concentration of glucose and ascorbic acid was about 10-folds that of diclofenac.

Detection of diclofenac containing impurities using modified electrode: The solution to be tested is 2 mL PBS buffer solution + 100 µL impurity ion (molecule) solution + 100 µL diclofenac solution (1 mM or 10 mM diclofenac solution selected according to the impurity concentration). At the end of the test, the change in peak current is analyzed and compared with the peak current of pure diclofenac detection. The percentage change in peak current is calculated and analyzed.

### 3. RESULTS AND DISCUSSION

The effect of the prepared gold nanoparticles on the electrochemical detection of diclofenac at different synthesis temperatures was investigated. Firstly, the prepared glassy carbon electrode was modified with gold nanoparticles at different temperatures, and the electrode performance and

impedance were tested in potassium chloride/potassium ferricyanide solution and compared with the unmodified glassy carbon electrode [21,22]. The experimental results are shown in Figure 1 and Figure 2. It can be seen from Figure 1 that the performance of the modified electrode is reduced, and the difference in peak potential is significant. It can be seen from Figure 1 that the performance of the modified electrode has decreased, and the peak-peak separation has become more extensive.

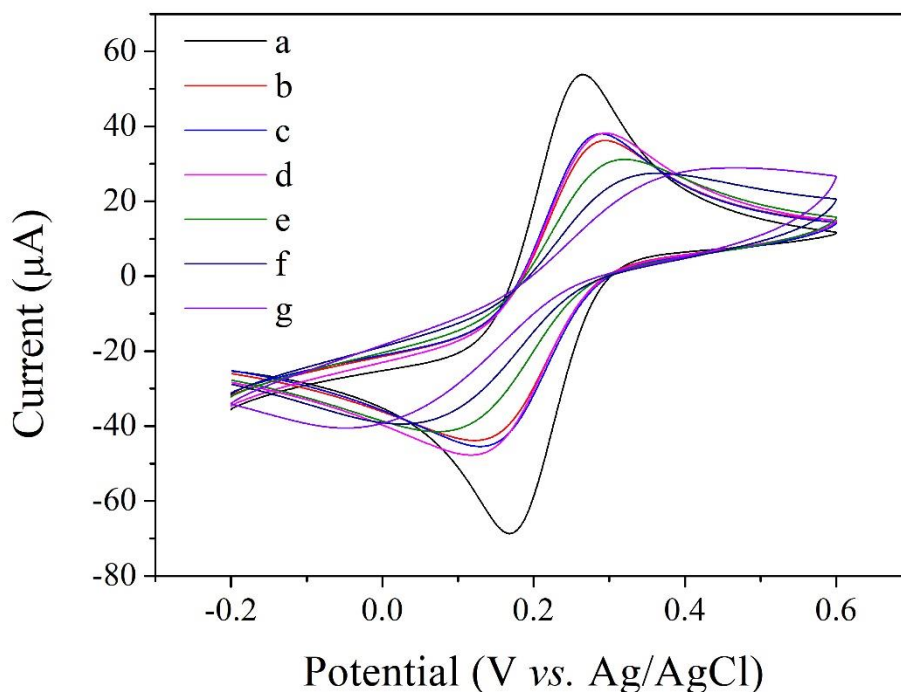


**Figure 1.** Cyclic voltammetry in KCl/K<sub>3</sub>[Fe(CN)<sub>6</sub>] solution for the glassy carbon electrode and gold nanoparticle modified electrode (a) Glassy carbon electrode (b) Biosynthesized gold nanoparticle (30°C) modified electrode (c) Biosynthesized gold nanoparticle (60°C) modified electrode (d) Biosynthesized gold nanoparticle (90°C) modified electrode (e) Biosynthesized gold nanoparticle (120°C) modified electrode (f) Biosynthesized gold nanoparticle (150°C) modified electrode (g) Biosynthesized gold nanoparticle (180°C) modified electrode.

The electrode performance of the gold nanomaterials modified electrode with the synthesis temperature below 100 °C is comparable to that of the bare electrode. The electrode performance of the gold nanomaterials modified electrodes synthesized above 100 °C differed significantly from that of the bare electrode, and the electrode performance decreased with increasing temperature. From the EIS plots in Figure 2, the impedance of the electrodes becomes larger as the synthesis temperature increases, and all of them are much larger than that of the bare electrode.

In the detection of diclofenac using CV, it can be found in Figure 3 that the peak current of diclofenac measured by the modified glassy carbon electrode is significantly higher than that of the bare electrode. When the synthesis temperature was lower than 100 °C, there was no significant difference in the performance of the electrodes with different temperature modifications for detecting diclofenac. However, the detection performance improved with the temperature increase after the synthesis

temperature was higher than 100 °C. Also, it can be seen from the figure that the peak of the modified electrode for the detection of diclofenac is shifted in the right direction [23]. In summary, the performance of the modified electrode itself is not ideal. The possible reason for this is that the prepared gold nanoparticles are coated with many plant molecules on the surface, leading to a decrease in the material's electrical conductivity. This makes the conductivity of the modified electrode also decrease. However, it may also be due to the adsorption of plant molecules on the surface of the gold nanoparticles that the modified electrode shows specificity in detecting diclofenac [24]. However, it may also be due to the adsorption of plant molecules on the surface of the gold nanoparticles that the modified electrode shows specificity in detecting diclofenac.

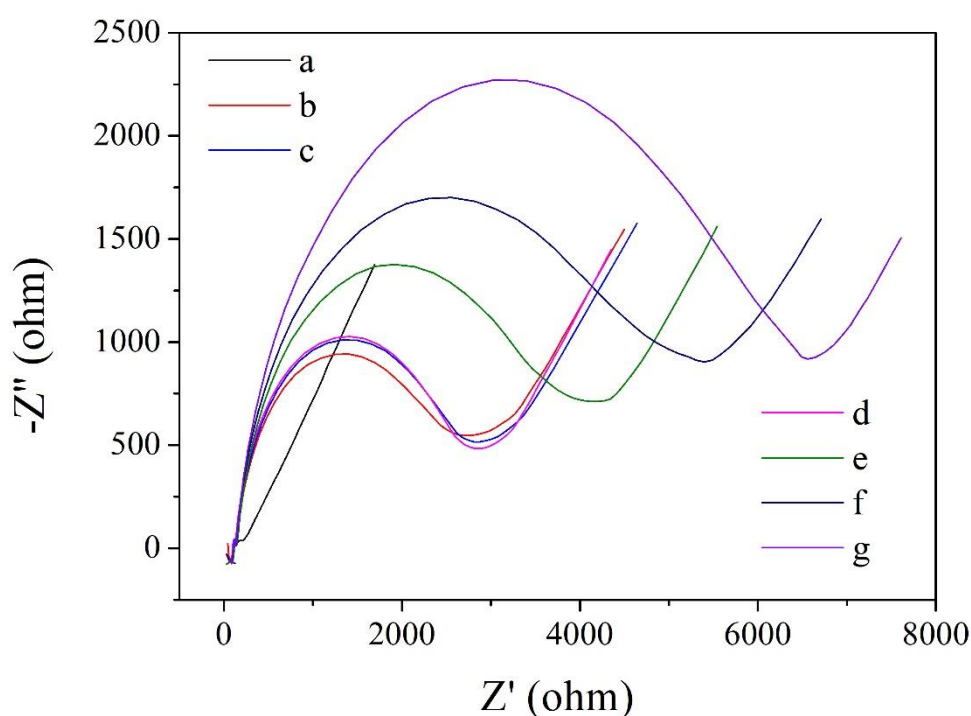


**Figure 2.** EIS in  $\text{KCl}/\text{K}_3[\text{Fe}(\text{CN})_6]$  solution for the glassy carbon electrode and gold nanoparticle modified electrode (a) Glassy carbon electrode (b) Biosynthesized gold nanoparticle (30°C) modified electrode (c) Biosynthesized gold nanoparticle (60°C) modified electrode (d) Biosynthesized gold nanoparticle (90°C) modified electrode (e) Biosynthesized gold nanoparticle (120°C) modified electrode (f) Biosynthesized gold nanoparticle (150°C) modified electrode (g) Biosynthesized gold nanoparticle (180°C) modified electrode.

We selected the sample with the best test performance synthesized at 180 °C and did SEM characterization, as shown in Figure 4A. It can be observed that the gold nanoparticles prepared by green synthesis are spherical. Moreover, from the morphology in the figure, the gold nanoparticles are mostly agglomerated, so the material should be dispersed when used. In all subsequent experiments, we performed ultrasonic dispersion of gold nanoparticles to make the gold nanoparticles uniformly dispersed in the solution and minimize the errors in the modification [25].

We performed the particle size analysis of the synthesized gold nanoparticles, and the results are shown in Figure 4B. The particle sizes of the synthesized gold nanoparticles were mainly distributed between 50 and 100 nm and had a Gaussian distribution by fitting analysis. The maximum particle size of some of the analyzed particles was 166.46 nm, the minimum particle size was 55.83 nm, and the average particle size was 87.45 nm.

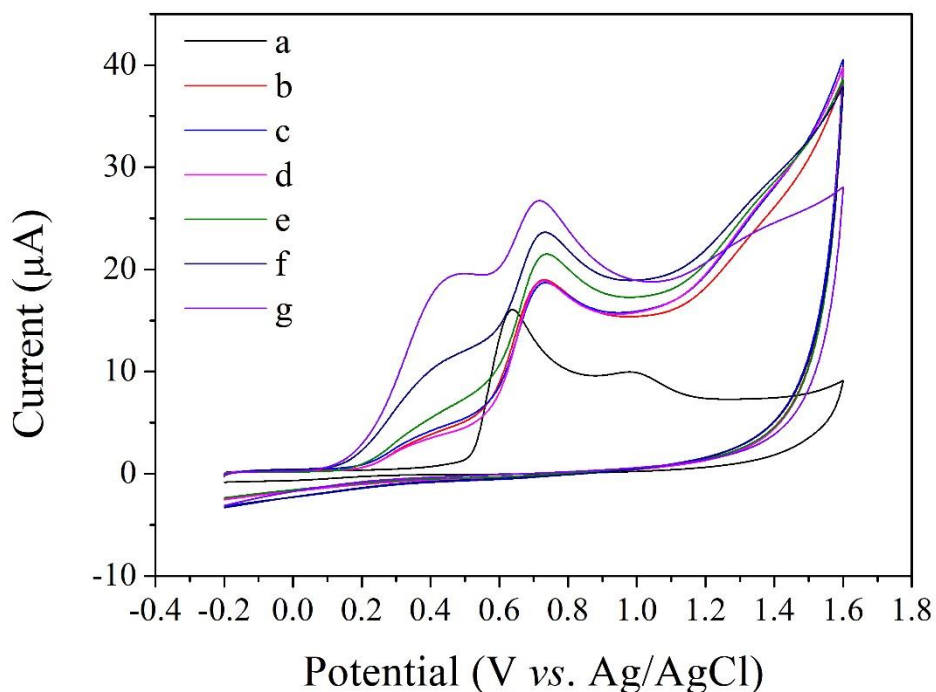


**Figure 3.** CV curves of (a) Glassy carbon electrode (b) Biosynthesized gold nanoparticle (30°C) modified electrode (c) Biosynthesized gold nanoparticle (60°C) modified electrode (d) Biosynthesized gold nanoparticle (90°C) modified electrode (e) Biosynthesized gold nanoparticle (120°C) modified electrode (f) Biosynthesized gold nanoparticle (150°C) modified electrode (g) Biosynthesized gold nanoparticle (180°C) modified electrode in PBS/diclofenac solution.

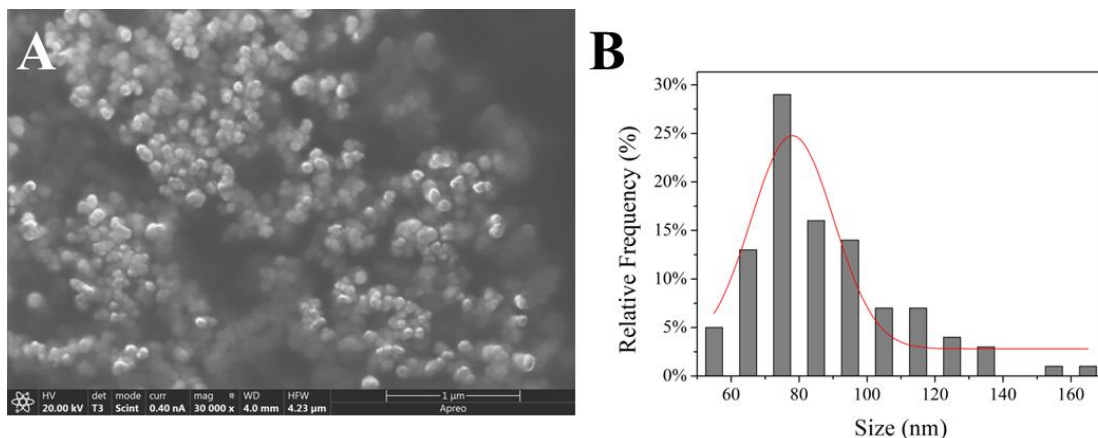


**Figure 4.** (A) SEM morphology and (B) Size distribution of gold nanoparticles synthesized at 180 °C.

The prepared gold nanoparticles needed to be modified onto the glassy carbon electrode in the experiment, so the modification amount was optimized. The effect of different volumes of modification on the electrochemical detection of diclofenac was examined. The effect of 0  $\mu\text{L}$ , 1  $\mu\text{L}$ , 3  $\mu\text{L}$ , 5  $\mu\text{L}$ , 7  $\mu\text{L}$ , and 9  $\mu\text{L}$  of modifier is shown in Figure 5, and it can be found that the detection effect increases with the increase of the amount of modifier. However, the peak shape also became less obvious after the increase in the amount of modifier, and the characteristic peak of diclofenac tended to be overlapped by other spurious peaks [26].

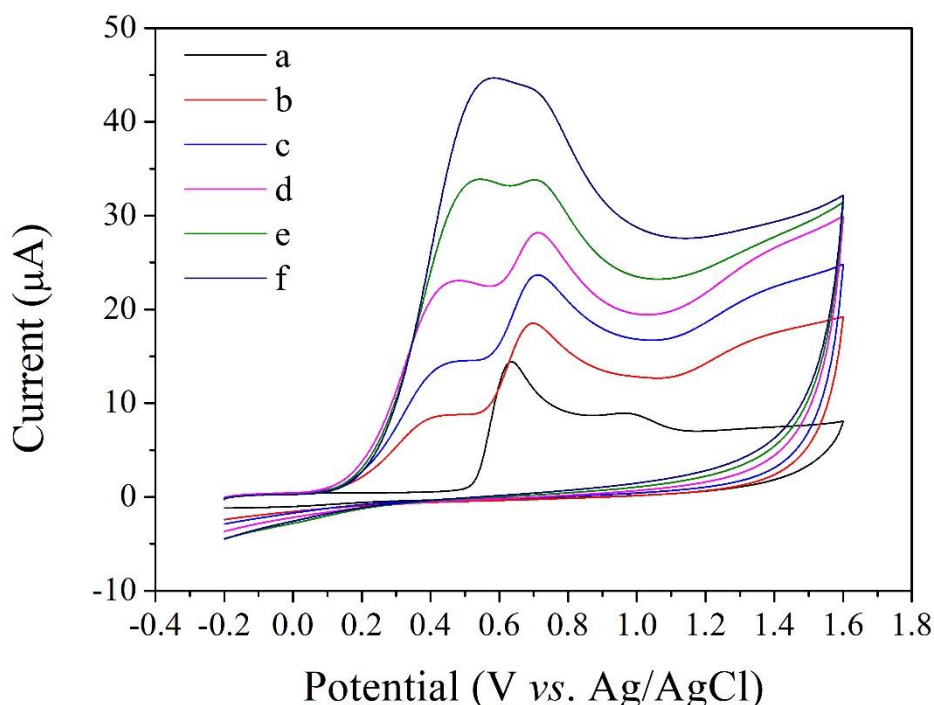


**Figure 5.** Cyclic voltammetry of diclofenac at glassy carbon electrodes with different amount of biosynthesized gold nanoparticle dispersion: (a) 0  $\mu\text{L}$ ; (b) 1  $\mu\text{L}$ ; (c) 3  $\mu\text{L}$ ; (d) 5  $\mu\text{L}$ ; (e) 7  $\mu\text{L}$ ; (f) 9  $\mu\text{L}$ .

Moreover, modifications above 5  $\mu\text{L}$  require multiple operations, which can lead to a specific chance of failure of the modification process. The effect of modifications above 10  $\mu\text{L}$  on detecting diclofenac was also examined. It was found that the detection effect was indeed more prominent for modification amounts higher than 10  $\mu\text{L}$ , but the peak shape became more rounded and the detection results were not stable. It was also found that the increase of the modification volume would come off from the surface of the glassy carbon electrode more efficiently, affecting the experimental results [27]. Considering the operability and the experimental results, a volume of 5  $\mu\text{L}$  was chosen as the modification volume for the subsequent experiments.

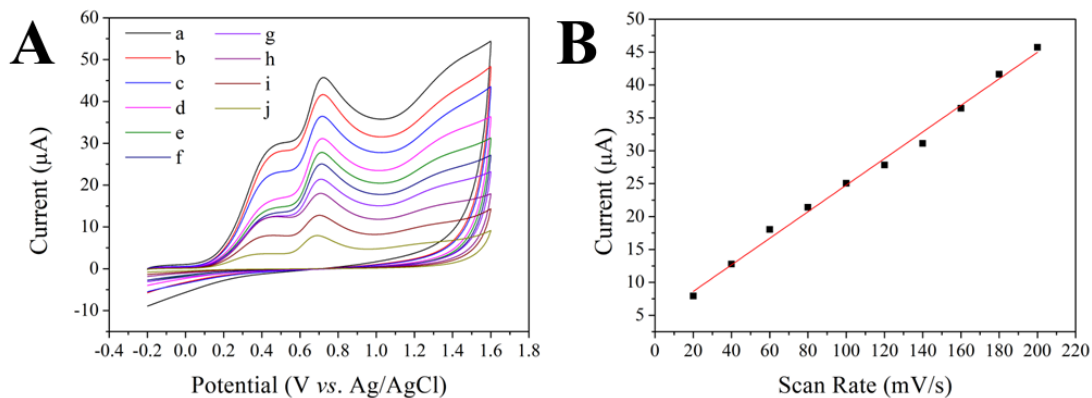


**Figure 6.** (A) Effect of different sweep rates on diclofenac detection. (a) 200 mV/s; (b) 180 mV/s; (c) 160 mV/s; (d) 140 mV/s; (e) 120 mV/s; (f) 100 mV/s; (g) 80 mV/s; (h) 60 mV/s; (i) 40 mV/s; (j) 20 mV/s. (B) Linear fit of sweep rate to peak current.

In electrochemical detection, the scan rate significantly influences the results. The test was scanned from high sweep rate to low sweep rate, and the experimental results are shown in Figure 6A. An increase in scan rate causes the peak to increase, and the oxidation potential shifts slightly to the right. A linear fit analysis of the relationship between scan rate and the peak current is shown in Figure 6B, where the peak current ( $I$ ) is proportional to the scan rate ( $v$ ). The linear fit results showed a linear fit equation of  $I=4.59107+0.2019v$  with a correlation coefficient  $R^2$  of approximately 0.993. The linear fit is more satisfactory, and the fit results indicate that the reaction process is controlled by the adsorption process rather than diffusion. When the scan rate is too fast, the results of multiple scans may be less stable. Conversely, when the scan rate is too slow, the peak current is not large enough, and the peak pattern for detection is not apparent enough. Therefore, we selected a scan rate of 100 mV/s for subsequent experiments.

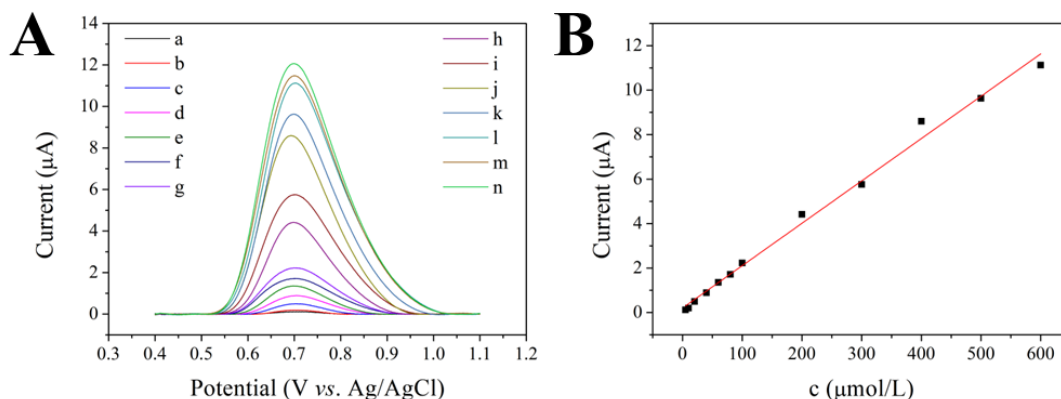


**Figure 7.** (A) DPV of modified electrode towards different concentrations of diclofenac. (a)  $c=5 \mu\text{M}$ ; (b)  $c=10 \mu\text{M}$ ; (c)  $c=20 \mu\text{M}$ ; (d)  $c=40 \mu\text{M}$ ; (e)  $c=60 \mu\text{M}$ ; (f)  $c=80 \mu\text{M}$ ; (g)  $c=100 \mu\text{M}$ ; (h)  $c=200 \mu\text{M}$ ; (i)  $c=300 \mu\text{M}$ ; (j)  $c=400 \mu\text{M}$ ; (k)  $c=500 \mu\text{M}$ ; (l)  $c=600 \mu\text{M}$ ; (m)  $c=700 \mu\text{M}$ ; (n)  $c=800 \mu\text{M}$ . (B) Linear fit of concentration of diclofenac to peak current.

The detection limits of diclofenac at the green synthetic gold nanoparticle modified electrode of *Ginkgo biloba* extract were examined. The experiments were performed from low to high concentrations

with 19 concentrations. Among them, 0.01 to 1  $\mu\text{M}$  concentrations were too low to be detected. The results of DPV detection for concentrations ranging from 5 to 800  $\mu\text{M}$  diclofenac are shown in Figure 7A. After processing and analyzing the data, a linear fit was done for each concentration's peak potential (I) versus concentration (c), as shown in Figure 7B. The linear fit equation was  $I=0.20468+0.01904c$  with a correlation coefficient  $R^2$  of 0.9927. The experimentally measured linear detection range was 5 to 600  $\mu\text{M}$ , and the calculated detection limit was 0.524  $\mu\text{M}$  (signal-to-noise ratio  $S/N=3$ ). Table 1 shows the performance of diclofenac detection using various electrochemical sensor. It can be seen that the proposed sensor showed a competitive performance.

**Table 1.** Sensing performance comparison of electrochemical sensors towards diclofenac detection.

Sensor	LDR	LOD	Reference
Amino-labeled aptamer/DCF/GCE	5 to 1000 $\mu\text{M}$	0.27 $\mu\text{M}$	[28]
$\beta$ -cyclodextrin	50 to 5000 $\mu\text{M}$	40 $\mu\text{M}$	[29]
Imidazolium	10 to 1000 $\mu\text{M}$	9.79 $\mu\text{M}$	[30]
Ni(II) bathophenanthroline	50 to 1000 $\mu\text{M}$	23 $\mu\text{M}$	[31]
Graphite	8.19 to 111 $\mu\text{M}$	2.45 $\mu\text{M}$	[32]
Biosynthesized AuNPs/GCE	0.01 to 1 $\mu\text{M}$	0.524 $\mu\text{M}$	This work

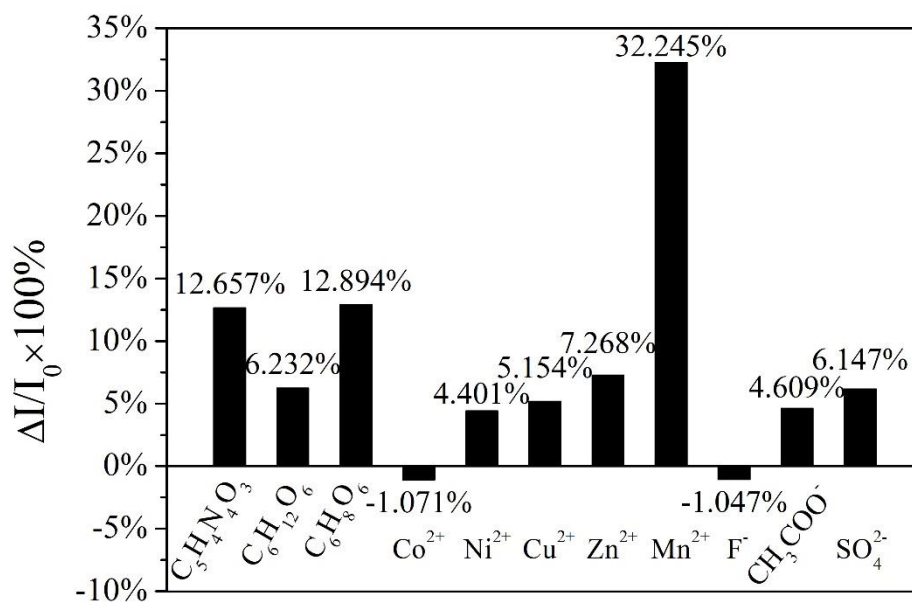


**Figure 8.** Effect of impurity ions (molecules) on the detection of diclofenac.

A total of 11 substances were tested in the anti-interference test. The DPV test showed that the detection peaks of most of the substances were not detected in the detection range of diclofenac, and only the detection peak of ascorbic acid was detected. The peak potential of ascorbic acid was around

0.26 V, while the detection peak of diclofenac was around 0.7 V. Therefore, none of the above impurity ions (molecules) affected the qualitative detection of diclofenac. The effect of the above impurity ions (molecules) on the gold nanoparticle modified electrode's peak current for detecting diclofenac is shown in Figure 8. The peak currents of diclofenac detected after adding impurities were analyzed, and the percentage of current change ( $\Delta I$ ) concerning the current value without impurities ( $I$ ) was calculated. The effect of  $\text{Co}^{2+}$  and  $\text{F}^-$  on the detection of diclofenac was minimal, at about 1%. The effects of glucose,  $\text{Ni}^{2+}$ ,  $\text{Zn}^{2+}$ ,  $\text{Cu}^{2+}$ ,  $\text{CH}_3\text{COO}^-$  and  $\text{SO}_4^{2-}$  on detecting diclofenac were minor and below 10%. The effect of uric acid and ascorbic acid on detecting diclofenac was slightly more significant, about 12% to 13%.  $\text{Mn}^{2+}$  had the most significant effect on detecting diclofenac, exceeding 30%. In summary, none of the impurities measured affected the detection of the characteristic peak of diclofenac, but all of them influenced the current value of the characteristic peak of diclofenac. Therefore, the impurity ions or molecules with more significant influence should be considered when performing quantitative assays.

#### 4. CONCLUSION

In this experiment, gold nanoparticles were prepared by green reduction using Ginkgo biloba extract, and their application in the electrochemical detection of diclofenac was investigated, and the following conclusions were drawn.

(1) The synthesis temperature has a particular influence on the preparation of gold nanoparticles. When the synthesis temperature was below 100 °C, the gold nanoparticle modified electrode performance was not much different, but the performance was lower than that of the bare electrode. When the synthesis temperature was above 100 °C, the gold nanoparticle modified electrode performance worsened with increasing synthesis temperature, but the detection of diclofenac became better with increasing temperature.

(2) SEM characterization showed that the synthesized gold nanomaterials were spherical, and the particle size was mainly distributed between 50 and 100 nm.

(3) The parameters were optimized for the electrochemical detection of diclofenac. The optimization parameters include the modification volume and the scan rate. The final experiment selected a modification volume of 5  $\mu\text{L}$  and a scan rate of 100 mV/s. The peak current is proportional to the scan rate, so the adsorption process controls the electrode response.

(4) The electrochemical detection limit and linear detection range of the prepared gold nanoparticle modified glassy carbon electrode for diclofenac were tested. The detection limit of 0.524  $\mu\text{M}$  and the linear detection range of 5~600  $\mu\text{M}$  were calculated.

(5) Interference experiments were conducted to detect the effects of impurity ions or impurity molecules on the electrochemical detection of diclofenac at gold nanoparticle-modified electrodes. The results showed that the effects of  $\text{Co}^{2+}$ ,  $\text{F}^-$ ,  $\text{Ni}^{2+}$ ,  $\text{Zn}^{2+}$ ,  $\text{Cu}^{2+}$ ,  $\text{CH}_3\text{COO}^-$ ,  $\text{SO}_4^{2-}$ , and glucose on detecting diclofenac were relatively small, and the effects were below 10%. The effect of uric acid and ascorbic acid on detecting diclofenac was slightly more significant, about 12%-13%. The effect of  $\text{Mn}^{2+}$  on detecting diclofenac was the greatest, over 30%.

## References

1. X. Wang, X. Zhong, J. Li, Z. Liu, L. Cheng, *Chem. Soc. Rev.*, 50 (2021) 8669–8742.
2. N. Baig, I. Kammakakam, W. Falath, *Mater. Adv.*, 2 (2021) 1821–1871.
3. S.A. Mazari, E. Ali, R. Abro, F.S.A. Khan, I. Ahmed, M. Ahmed, S. Nizamuddin, T.H. Siddiqui, N. Hossain, N.M. Mubarak, *J. Environ. Chem. Eng.*, 9 (2021) 105028.
4. S.H.M. Taib, K. Shameli, P.M. Nia, M. Etesami, M. Miyake, R.R. Ali, E. Abouzari-Lotf, Z. Izadiyan, *J. Taiwan Inst. Chem. Eng.*, 95 (2019) 616–626.
5. M.P. Patil, E. Bayaraa, P. Subedi, L.L.A. Piad, N.H. Tarte, G.-D. Kim, *J. Drug Deliv. Sci. Technol.*, 51 (2019) 83–90.
6. S. Balasubramanian, S.M.J. Kala, T.L. Pushparaj, *J. Drug Deliv. Sci. Technol.*, 57 (2020) 101620.
7. Y. Huang, C.Y. Haw, Z. Zheng, J. Kang, J. Zheng, H. Wang, *Adv. Sustain. Syst.*, 5 (2021) 2000266.
8. N. Singh, P. Jain, A. De, R. Tomar, *Curr. Pharm. Biotechnol.*, 22 (2021) 1705–1747.
9. A. Nande, S. Raut, M. Michalska-Domanska, S.J. Dhoble, *Curr. Pharm. Biotechnol.*, 22 (2021) 1794–1811.
10. Z. Karavelioglu, R. Cakir-Koc, *Int. J. Biol. Macromol.*, 192 (2021) 675–683.
11. Z. Zhang, G. Hao, G. Zhang, D. Hu, Q. Li, R. Cao, M. Hao, *J. Nanomater.*, 2021 (2021) 6647593.
12. M. Mostafavi, M.R. Yafthian, F. Piri, H. Shayani-Jam, *Biosens. Bioelectron.*, 122 (2018) 160–167.
13. C. Zhang, Z. Cao, G. Zhang, Y. Yan, X. Yang, J. Chang, Y. Song, Y. Jia, P. Pan, W. Mi, Z. Yang, J. Zhao, J. Wei, *Microchem. J.*, 158 (2020) 105237.
14. H.A. Almashhadani, M.K. Alshujery, M. Khalil, M.M. Kadhemi, A.A. Khadom, *J. Mol. Liq.*, 343 (2021) 117656.
15. N.C. Honakeri, S.J. Malode, R.M. Kulkarni, N.P. Shetti, *Sens. Int.*, 1 (2020) 100002.
16. V. Prakash, M.C. Bishwakarma, A. Chaudhary, R. Cuthbert, R. Dave, M. Kulkarni, S. Kumar, K. Paudel, S. Ranade, R. Shringarpure, *PLoS One*, 7 (2012) e49118.
17. W. Boumya, N. Taoufik, M. Achak, H. Bessbousse, A. Elhalil, N. Barka, *Talanta Open*, 3 (2021) 100026.
18. S. Motoc, F. Manea, C. Orha, A. Pop, *Sensors*, 19 (2019) 1332.
19. M.M. Eteya, G.H. Rounaghi, B. Deiminiat, *Microchem. J.*, 144 (2019) 254–260.
20. Md. Shalauddin, S. Akhter, W.J. Basirun, S. Bagheri, N.S. Anuar, Mohd.R. Johan, *Electrochimica Acta*, 304 (2019) 323–333.
21. G. Venkataprasad, T.M. Reddy, A.L. Narayana, O. Hussain, P. Shaikshavali, T.V. Gopal, P. Gopal, *Sens. Actuators Phys.*, 293 (2019) 87–100.
22. J.G. Pacheco, P. Rebelo, M. Freitas, H.P. Nouws, C. Delerue-Matos, *Sens. Actuators B Chem.*, 273 (2018) 1008–1014.
23. T. Anirudhan, J. Deepa, *Mater. Sci. Eng. C*, 92 (2018) 942–956.
24. B. Feier, A. Blidar, A. Pusta, P. Carciuc, C. Cristea, *Biosensors*, 9 (2019) 31.
25. F. Zouaoui, S. Bourouina-Bacha, M. Bourouina, N. Jaffrezic-Renault, N. Zine, A. Errachid, *TrAC Trends Anal. Chem.*, 130 (2020) 115982.
26. A. Sinha, P.K. Kalambate, S.M. Mugo, P. Kamau, J. Chen, R. Jain, *TrAC Trends Anal. Chem.*, 118 (2019) 488–501.
27. Y. He, L. Ma, L. Zhou, G. Liu, Y. Jiang, J. Gao, *Nanomaterials*, 10 (2020) 866.
28. L. Kashefi-Kheyraadi, M.A. Mehrgardi, *Biosens. Bioelectron.*, 33 (2012) 184–189.
29. J. Lenik, *Mater. Sci. Eng. C*, 45 (2014) 109–116.
30. E. Brennan, P. Futvoie, J. Cassidy, B. Schazmann, *Int. J. Environ. Anal. Chem.*, 97 (2017) 588–596.
31. S. Saad, *Analyst*, 119 (1994) 1993–1996.

32. G.Y. Aguilar-Lira, G.A. Álvarez-Romero, A. Zamora-Suárez, M. Palomar-Pardavé, A. Rojas-Hernández, J.A. Rodríguez-Ávila, M.E. Páez-Hernández, *J. Electroanal. Chem.*, 794 (2017) 182–188.

© 2022 The Authors. Published by ESG ([www.electrochemsci.org](http://www.electrochemsci.org)). This article is an open access article distributed under the terms and conditions of the Creative Commons Attribution license (<http://creativecommons.org/licenses/by/4.0/>).